Fly ash as reactive sorbent for phosphate removal from treated waste water as a potential slow release fertilizer

M. Hermassi [a,b], C. Valderrama[a], N. Moreno[c], O. Font[c], X. Querol[c], N.H. Batis[b] and J.L. Cortina[a]

[a]Chemical Engineering Department. Universitat Politècnica de Catalunya-Barcelona TECH

[b]Department of Biological and Chemical Engineering, National Institute of Applied Sciences and Technology (INSAT), University of Carthage (Tunisia)

[c]Institute of Environmental Assessment and Water Research IDAEA, Consejo Superior de Investigaciones Científicas (CSIC) Barcelona

*Correspondence should be addressed to: Mehrez Hermassi

Departament d'Enginyeria Química, Universitat Politècnica de Catalunya

Av. Diagonal 647, 08028 Barcelona, Spain

Tel.: 93 4011818, Fax.: 93 401 58 14

Email: mehrez.harmassi@upc.edu;

Abstract

There is interest in recovering phosphate (P(V)) from secondary sources, such as waste water streams for potential use as fertilizers reducing the environmental impacts of P(V) discharges and providing alternative phosphorus sources. The goal of this work was to provide an understanding of P(V) removal by fly ash (FA) from coal power plants. Phosphate removal using Ca(II) rich FA was evaluated in terms of i) sorption equilibrium, ii) sorption kinetics under the expected pH values and P(V) concentrations in wastewaters effluents, and iii) P(V) availability of the FAs in agricultural applications. At the pH values (6 to 9) expected for wastewater effluents, P(V) removal proceeds as a combination of CaO(s) dissolution and brushite ($CaHPO_4$(s)) formation on the FA particles. This process avoids the formation of relatively insoluble Ca–phosphates, such as, hydroxyapatite (Hap) with limited fertilizing properties. High P-

loadings were achieved (up to 50 mgP-PO_4/g FA (5% P(V) by weight)) at a pH of 8. The removal kinetics data were well described as a diffusion-based process of phosphate ions ($H_2PO_4^-$ and HPO_4^{2-}) on FA particles, and the CaO(s) dissolution process was discarded as the rate controlling step. The P(V) availability from loaded samples was determined via an agronomical assay with $NaHCO_3$ solutions with P(V) release ratios of 10 to 30 mgP-PO_4/g in FA, confirming the appropriateness of this material as a potential fertilizer, even in calcareous soils.

Keywords: P(V), phosphate recovery; sorption; fly ash; brushite; slow release fertilizer

1. Introduction

Increasing energy demands worldwide have led to increased utilisation of coal and, thus, the production of large quantities of fly ash (FA) as a waste product [1–3]. In 2011, coal-fired generation accounted for 30% of the world's electricity supply, and its share is anticipated to reach 46% by 2030. Sustained prices for oil and natural gas make coal-fired generation relatively economically attractive, particularly in nations with rich coal resources, such as China, the USA and India [4,5]. Recycling coal fly ash (CFA) can be a good alternative disposal method and could provide significant economic and environmental benefits. The global average FA utilisation ratio is estimated to be nearly 25% [6,7]. Most FA is alkaline, and its surface is negatively charged at high pH values; thus, it could be used to remove metal ions from solutions by precipitation [8] or sorption [3,8,9]. Furthermore, it contains a certain amount of unburnt carbon, which has a high adsorption capacity for organic compounds [5].

Phosphorous (P) is an important element in industry and agriculture and is frequently present in domestic, industrial, and farming wastewaters. In the last decades, phosphate has been considered an environmental concern because of its role in the eutrophication of water bodies [10,11]. Currently, it is becoming increasingly economically concerning because its natural deposits are diminishing because of the continuous growth of the world population. Then, such wastewaters and sludge containing P (less than 1% by weight) are considered secondary P sources that should be mined [12]. In the European

Union, P has been included in the list of Critical Elements, and new technologies to recover P from secondary sources are being promoted. Most of these technologies have focused on the recovery of P from solid wastes (e.g., incineration ashes), whereas for its recovery from liquid wastes, most technologies have focused on the recovery of struvite (MAP) from concentrated streams.

Few efforts have been devoted to P recovery from diluted streams, although various removal techniques are available [13]. Chemical precipitation and coagulation processes are not cost effective and polymeric ion exchangers are not applicable because of the presence of dissolved and particulate organic matter. Thus, phosphate-removal/recovery solutions have focused on the use of low-cost inorganic materials with high performance in terms of equilibrium and kinetics. CFA has attracted substantial attention as a potential material for phosphate removal because it is easily available and cost effective [14–16]. The presence of aluminium, iron, calcium and magnesium oxides imbues FA with suitable properties for phosphate removal by complexation or precipitation of Ca/Mg-phosphates [3,17]. Cheung and Venkitachalam [18] associated the removal of phosphate by FA containing high- and low-calcium contents with Ca-phosphate precipitation. Johansson and Gustafsson [19] proposed the formation of amorphous calcium phosphate and/or octacalcium phosphate as the major P-removal mechanism and suggested the direct formation of hydroxyapatite (Hap) as the predominant removal mechanism. Although it is generally accepted that phosphate removal by FA involves adsorption and/or precipitation mechanisms, the interaction between phosphate and Ca(II) remains incompletely described [12].

Additionally, reduced progress has been done to obtain a solution for the exhausted ash, and recently, the possibility of using this material to improve the soil quality of areas degraded or for forestry applications has been proposed [5]. However, because of the low solubility and bio-availability of the Ca-phosphate mineral that is typically precipitated ($Ca_5(PO_4)_3OH$(s), $\log K_{so}$=116.8) [20], efforts have been made to prepare more soluble minerals, such as brushite ($CaHPO_4.2H_2O$, $\log K_{so}$=6.59) [21]) with properties suitable as slow-release fertilizers. These materials include Ca-silicates, such as wollasonite

[22]; Ca-Al layered double hydroxide [23,24]; natural zeolites [25]; and FA [26]. However, the utilisation of powdered inorganic adsorbents for selective P removal and its potential use as slow-release fertilizers remain under development.

In this study, two different types of FA from two coal power stations with different CaO(s) contents (Los Barrios (FA-LB (2.8% w)) and Teruel (FA-TE (4.8% w))) were evaluated as adsorbents for phosphate recovery. The equilibrium and kinetic performances for phosphate sorption were studied and characterised by varying the experimental conditions, such as the solution pH and initial phosphate concentration. The phosphate-sorption mechanism was evaluated using a speciation method. Although the phosphate-removal mechanism is complex, the results are presented in terms of equilibrium isotherms and kinetic parameters.

2. Materials and methods

2.1 Batch equilibrium experiments of FA dissolution

FA samples (0.2 g) were mechanically mixed in polyethylene tubes with deionised water (10 mL) at different initial pH values (6-9) and at room temperature (21±1 °C) until equilibrium was achieved. The influence of the initial pH on FA dissolution was evaluated by varying the initial pH with 0.1-mol/L HCl or NaOH solution. After phase separation with a 0.2-µm syringe filter, the equilibrium pH was measured using a pH glass electrode (Crison GLP22); the total Ca, Na, Mg, and K concentrations were measured by ion chromatography (Thermo Scientific Dionex ICS-1100); and the total Si, Al, Fe, P, and Ti concentrations were determined by Inductively Coupled Plasma Mass Spectrometry (ICP-MS) or Atomic Emission Spectrophotometry (ICP-AES) (X-Series II, Thermo Fisher SCIENTIFIC).

FA selection samples in this study (LB, TE) was based on having the highest Ca(II) and Mg content and the lowest toxic metallic and non-metallic traces. This selection was based on leaching studies for both samples that were published previously [27].

2.2 Batch equilibrium experiments of phosphate removal

Phosphate solutions were prepared by dissolving a weighed amount of $Na_2HPO_4.2H_2O$ in deionized water (Milli-Q-Academic-A10 apparatus). FA samples from Teruel (FA-TE) and Los Barrios (FA-LB) (0.2 g) were mechanically mixed in polyethylene tubes with an aqueous phosphate solution (10 mL) at different initial concentrations (100–16000 mgP-PO_4/L) at room temperature (21±1 ºC) until equilibrium was achieved. The influence of pH on the phosphate sorption was evaluated by varying the initial pH with 0.1 mol/L HCl or NaOH solution. After phase separation, the equilibrium pH was measured and the total phosphate concentration was measured by ion chromatography or by visible absorption spectrophotometry (UVmini-1240) [28]. The P(V) equilibrium sorption capacity was determined using Eq. 1.

$$q_e = \frac{(C_0 - C_e)\, v}{m_s} \quad (1)$$

where C_0 (mg/L) and C_e (mgP-PO_4/L) represent the initial and equilibrium total P(V) concentrations, respectively; v (L) is the aqueous solution volume; and m_s (g) is the mass of the FA sample.

2.3 Batch kinetic experiments of phosphate removal

Batch kinetic experiments were performed by adding of 0.2 g of FA to solutions containing 100 and 500 mgP-PO_4/L. The tubes were mechanically shaken at 21±1 °C, and samples were withdrawn sequentially at specified times. All tests were performed in triplicate and the average values are reported. The samples were centrifuged for 10 min and then filtered. The total phosphate concentration and pH of the initial and remaining aqueous solutions were measured.

2.4 Speciation of phosphate-loaded FA samples

The speciation of the adsorbed P in both FA samples (FA-TE and FA-LB) was achieved using a modified four-step sequential extraction methodology [29–31]. First, 30 mL aliquots of 1000 mg P-PO_4/L at pH 7 were equilibrated with pre-weighed tubes containing 3 g of FA. After shaking for 24 h at room temperature, the suspensions were centrifuged, and the FA powders were dried at 50-60°C. The

adsorbed phosphate was sequentially extracted using 1 g samples and 50 mL of the extraction solutions described in Table 1. The samples were mechanical shaken at 21 ±1°C. After equilibrium was achieved, the samples were centrifuged, and the phosphate content of the aqueous phase was analysed.

Table 1. Chemical extraction scheme for phosphorus speciation of loaded FA samples.

Extraction solutions	Speciation name	P Speciation	Step
40-mL 2 M KCl for 2h	KCl-P	Soluble and exchangeable P	1
40-mL 0.1 M NaOH for 17h	NaOH-P	Fe- and Al-bound P	2
40-mL 0.5 M HCl for 24h	HCl-P	Ca-bound P	3
40-ml 10 M HNO_3/10M $HClO_4$ (5/2)	Res-P	Residual P	4

2.5 Phosphate availability from loaded FA samples using bicarbonate solutions

Samples (0.5 g) of loaded FA samples (contents ranging from 11 to 108 mmol/L) were mixed with 20 mL of 0.5 M $NaHCO_3$ (pH=8.3) in 50 mL plastic bottles. The bottles were mechanically shaken at 21 ±1°C for 24 h at a constant agitation speed. After phase separation, with a 0.45 µm syringe filter, the equilibrium pH and total phosphate concentration were measured.

2.6 Physicochemical characterisation of FA samples

The major, minor, and trace element concentrations of the FA powders were determined. The samples were acid-digested via a special two-step digestion method to analyse the trace elements in coal and combustion wastes by ICP-MS and ICP-AES [32].

After the sorption and desorption experiments, the FA samples were washed with water to remove the interstitial water and then oven-dried at 60°C for structural and textural analysis. The mineralogical composition was analysed by a Bruker D8 A25 Advance X-Ray Diffractometer θ-θ with $CuK_{\alpha 1}$ radiation, Bragg-Brentano geometry, and a linear LynxEyeXE detector. The diffractograms were obtained from 4º to 60º of 2θ with a step size of 0.015º and a counting time of 0.1s as the sample was rotated. The solids

in powder form were identified according to standard Joint Committee on Powder Diffraction Standards (JCPDS) file and were matched with Powder Diffraction Files (PDFs) no. 009-0077 for brushite, 046-1045 quartz, 015-0776 mullite, 033-0664 for hematite, and 039-1346 for maghemite. The morphology of the samples was examined using field emission scanning electron microscopy with an energy dispersive system (FE-SEM-EDS, JEOL 3400) after prior metallisation with gold.

The FA point of zero charge (PZC) was determined by acid-based potentiometric titrations using the common intersection point method [33–35]. First, 0.1 g of FA was equilibrated with 25 mL of KNO_3 solution at various ionic strengths (0.01, 0.05, 0.1, and 0.5 M) at 21±1°C. After equilibrium was achieved, a given volume of 0.1 M KOH solution was added to the suspension to increase the pH value over 10. The suspension was then titrated with 0.05 M HNO_3 to pH≈3 using an automatic titrator (Mettler Toledo). The net surface charge was correlated with the PZC by considering the adsorbed amounts of H^+ and OH^- ions along the titration assay: the titration curves obtained at different ionic strengths intersect at $pH=pH_{PZC}$. The surface charge was calculated according to Eq. 2 [36].

$$b = C_b - C_a + [H^+] - [OH^-] \quad (2)$$

where b (mol/g) is the net amount of hydroxide ions consumed; C_b and C_a (mol/L) are the base and acid concentrations, respectively; and $[H^+]$ and $[OH^-]$ denote the proton and hydroxide concentrations, respectively, calculated from the measured pH for a given mass (g) of FA and a given volume of solution (L). All measurements were performed in triplicate, and the average values are reported.

2.7 Sorption models

Equilibrium models: Langmuir and Freundlich models were used to describe the sorption equilibrium data at constant pH. The Langmuir isotherm assumes monolayer sorption and only occurs at a finite number of definite localized sites. Furthermore, Langmuir isotherm refers to homogenous sorption, where all sites possess equal affinity for the sorbate as is described by the Eq. (3). The Freundlich

isotherm describes a heterogeneous and reversible sorption not restricted to the formation of a monolayer. The Freundlich equation is given by Eq. (4) [37,38].

$$\frac{C_e}{q_e} = \frac{1}{K_l q_m} + \frac{C_e}{q_m} \quad (3)$$

$$\log q_e = \log K_f + \frac{1}{n}\log C_e \quad (4)$$

where C_e (mg P-PO_4/L) and q_e (mg/g) are the equilibrium total P(V) concentrations in the aqueous and FA phases, respectively; q_m (mg P-PO_4/g) is the maximum sorption capacity; K_L (L/mg) is the Langmuir sorption equilibrium constant; n is a constant indicating the isotherm curvature; and K_f ((mg/g)/(mg/L)$^{1/n}$) is the Freundlich equilibrium constant. The adjustable parameters q_m and K_L or K_F and n were obtained by fitting the experimental data (q_e and C_e) to Eqs. 3 and 4 using nonlinear least squares regression (Excel version 2010).

Kinetic equilibrium models: The homogeneous particle diffusion (HPDM) and shell progressive (SPM) models were used to describe the kinetic data [39]. Both models assume that the extraction mechanism involves the diffusion of phosphate ions ($H_2PO_4^-$ and HPO_4^{2-}) from solution into the FA phase through a number of possible pathways: diffusion across the liquid film surrounding the FA particle, transfer across the solution/particle interface, diffusion into the bulk of the FA particle and possible interactions with reactive groups on the FA surface.

HPDM model describes the sorption of the phosphate ions via diffusion in a quasi-homogeneous medium according to Fick's law equation with two rate-control scenarios:

- If the particle diffusion rate controls the P(V) sorption on spherical FA particles:

$$-\ln(1 - X^2(t)) = 2Bt \qquad \text{where } B = \frac{\pi^2 D_e}{r^2}. \quad (5)$$

- If liquid film diffusion controls the rate of P(V) sorption:

$$-\ln\big(1 - X(t)\big) = K_{li}\, t \qquad \text{where } K_{li} = \frac{3D_e C}{r C_r} \quad (6)$$

The X(t) values can be calculated using Eq. 7:

$$X(t) = \frac{q_t}{q_e} \quad (7)$$

where X(t) is the phosphate fractional attainment of equilibrium at time t; q_t and q_e are the phosphate loadings on the FA phase at time t and when equilibrium is attained (mg/g), respectively; C is the total concentration of phosphate; C_r is the total concentration of phosphate in the FA; K_{li} is the rate constant for film diffusion ; D_e is the effective diffusion coefficient of phosphate ions in the FA (m^2/s); and r the radius of the FA particle, which is assumed to be spherical (m).

SPM model describes the sorption process in terms of a concentration profile of the solution containing phosphate ions advancing into a partially sorbed spherical FA particle ("Shell Progressive") where the relationships between phosphate sorption degree and time are given by Eqs. 7-9:

- if sorption is controlled by the fluid film:

$$X(t) = \frac{3C_{Ao}K_F}{a_S C_{so}}\ t \quad (8)$$

-if sorption is controlled by diffusion though the sorption layer:

$$\left[3 - 3(1 - X(t))^{\frac{2}{3}} - 2X(t)\right] = \frac{6D_e C_{Ao}}{a_s^2 C_{so}}\ t \quad (9)$$

- if sorption is controlled by the chemical reaction:

$$\left[1 - (1 - X(t))^{1/3}\right] = \frac{K_S C_{Ao}}{r}\ t \quad (10)$$

where a_s is the stoichiometric coefficient; C_{Ao} is the bulk phosphate concentration; C_{so} is the FA phosphate concentration, K_F is the mass-transfer coefficient of phosphate species through the liquid film (m/s) and K_s is a surface reaction constant (m/s).

All experimental data were treated graphically and compared to all fractional attainment of equilibrium functions (F(X) = f (t)) defined previously for both HPDM (Eqs. 5-6) and SPM (Eqs. 8-10).

2.8 Prediction of phosphate-precipitation processes

Phosphate-precipitation processes were studied using the HYDRA-MEDUSA [40] and Visual Minteq codes [41]. When necessary, the measured P(V), Ca(II) concentration and pH were compared to those estimated using both codes. The supersaturation index (SI) was calculated using Visual Minteq and Eq. 11, as indicated by Eq. 11:

$$SI = \log\left(\frac{IAP}{K_{so}}\right) \quad (11)$$

where IAP is the ion activity product and K_{so} is the solubility constant. Equilibrium solubility data for Ca-phosphates from the HYDRA and PHREEQ C databases were critically reviewed.

3. Results and discussion

3.1. Characterisation of the Teruel and Los Barrios FAs

The chemical compositions of both FA samples (Table 2) consist mainly of Al_2O_3 and SiO_2, which account for 73% and 83% of the FA-TE and FA-LB samples, respectively. FA-TE has a higher contents of Fe_2O_3 (18.9%) and CaO (4.2%) than FA-LB (with 7.4% and 2.3%, respectively). The X-ray diffraction (XRD) patterns of FA-TE and FA-LB are shown in Fig. 1a. Hematite and maghemite (Fe_2O_3), mullite ($Al_2Si_2O_{13}$) and quartz (SiO_2) were the main phases identified in both cases. SEM analysis identified spherical particles containing encapsulated smaller particles (Fig. 1b). Natusch and Taylor [42] classified five different types of particles according to the size or porous texture: i) spherical filled particles–Plerospheres in the particle size range below 10 μm; ii) large irregular silicate masses, exhibiting spherical pitting; iii) hollow spherical particles–Cenospheres containing small particles encapsulated inside them; iv) elongated blades and hollow spherical particles with interior voids and v) agglomerates of small spherical particles forming large non-spherical particles. For both samples only two types of morphologies, thin walled cenopheres and plerospheres were identified as it is shown in Fig. 1b.

Table 2. Average chemical composition of FA-TE and FA-LB fly ash samples.

	SiO_2	Al_2O_3	Fe_2O_3	CaO	MgO	Na_2O	K_2O	P_2O_5	SO_3
FA- TE (% wt)	45.1	28.1	18.9	4.2	1.2	0.2	1.5	0.2	0.8
FA- LB (% wt)	61.2	21.1	7.4	2.3	2.3	1.2	2.4	1.6	0.7

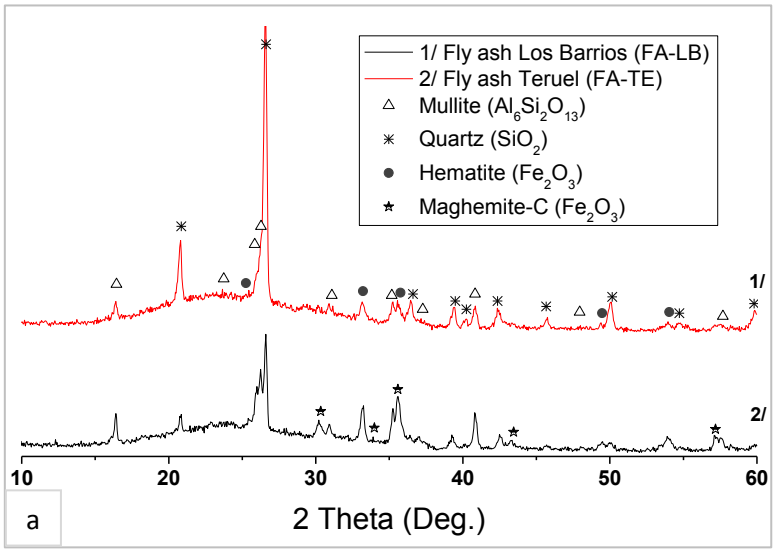

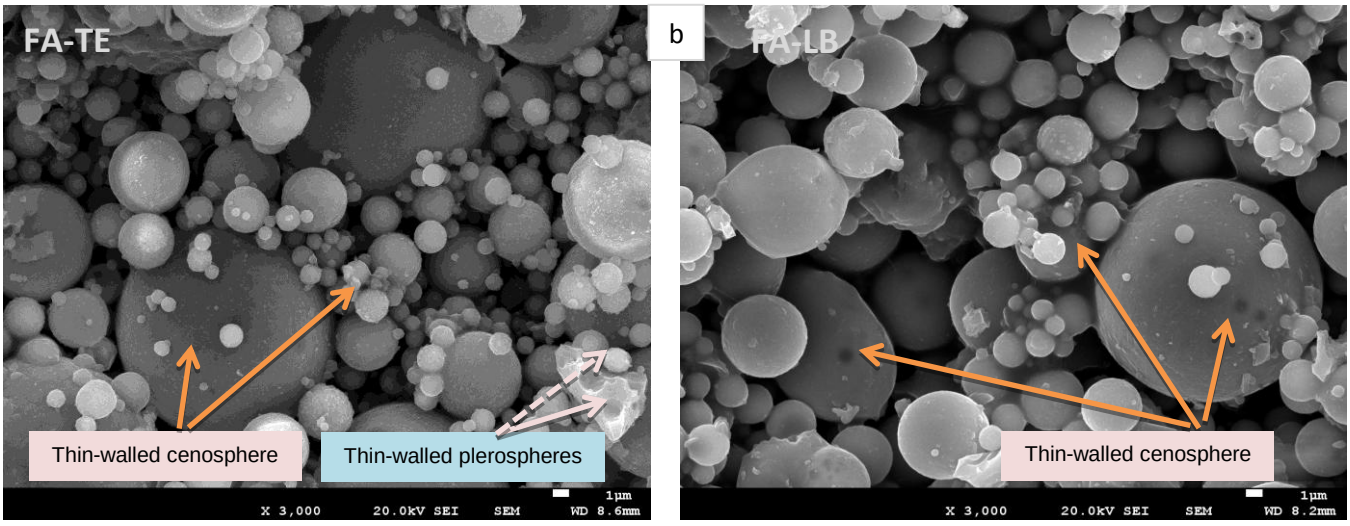

Figure 1. a) XRD patterns of both types of fly ash samples FA-TE; FA-LB and b) SEM analyses for FA-TE and FA-LB

FA samples selection for this study (FA-TE, and FA-LB) was based on the Ca(II) and Mg content and the toxic metallic and non-metallic traces content. This selection was supported on the leaching studies

for both samples that were published previously and summarised in the Table S1 (Supplementary material) [27]. As can be seen, the content of heavy metals (Pb, Cd, Hg) and non-metals (As) are lower (ng/g). Measured concentrations using standard leaching test in acidic conditions, show also concentration levels of those elements not statistically different to those present in domestic wastewaters. Indeed, in the expected pH values of treated waste waters (7 to 8.5), most of the potential leached metals/non-metals show their lower solubility values, although potential presence of complexing organic molecules could increase solubility.

The acid-base characterisation revealed a pH_{PZC} values of 4.9±0.5 for FA-TE and 5.1±0.5 for FA-LB (Fig. 2) The electrophoretic mobility (pH_{ZPC} value of approximately 4.9-5.1) is close to the theoretically predicted value and is reported in supporting material Table S2 (Supplementary material) [43] based on the percentages of silica and alumina in the FA.

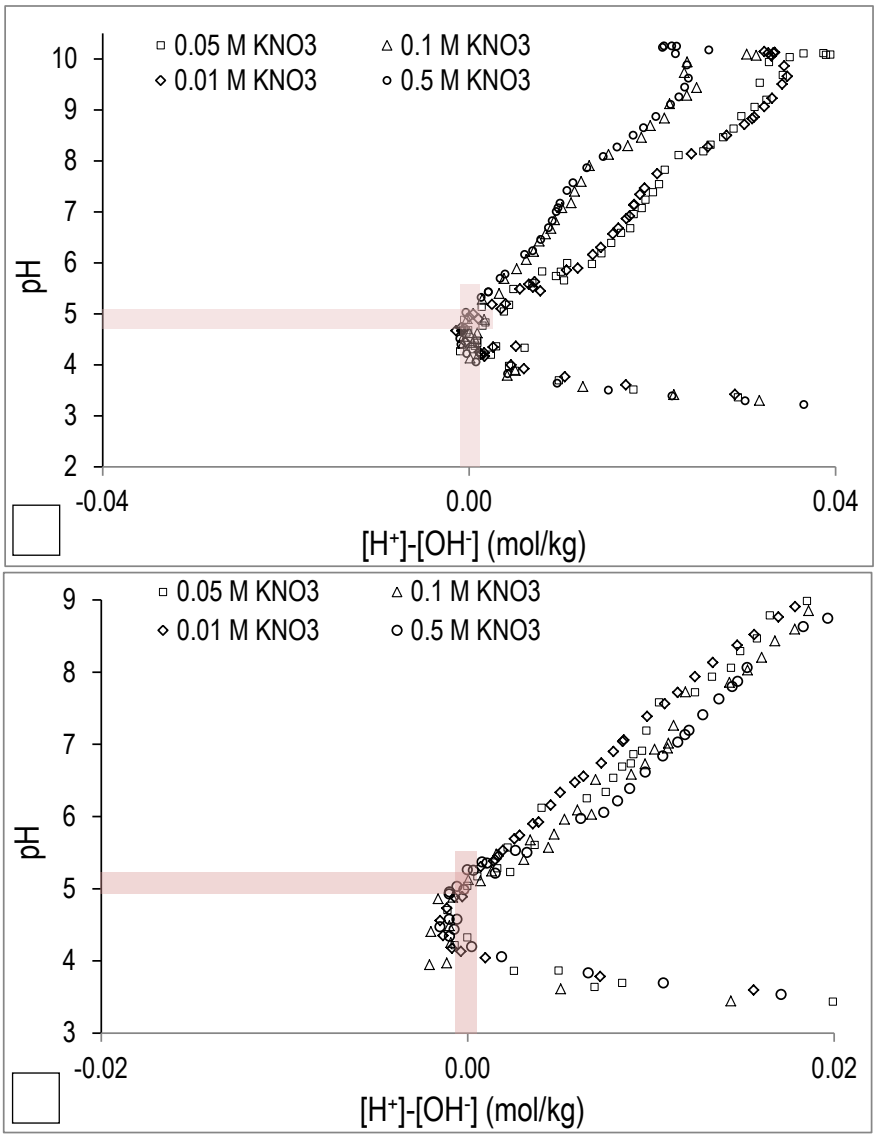

Figure 2. Fly ash potentiometric titration curve at 0.01, 0.05, 0.1, and 0.5 M KNO_3 for FA samples: a) FA-TE and b) FA-LB.

The deviation between the theoretical and experimental data is ascribed to the presence of other oxides in the FA samples (e.g., MgO and CaO). The determined pH_{PZC} values are in good agreement with those reported for α-$Al(OH)_3$(s) (pH_{PZC} 5.0) and $Fe(OH)_3$ (pH_{PZC} from 5 to 7) [44]. Indeed, Chen et al. and Zhang et al. [45–47] reported that, iron and aluminium surface groups at pH values below the pH_{PCZ} have anion sorption capacities.

FA dissolution experiments at initial pH values between 6 to 9 revealed Ca(II) concentration in solution of 2 to 3.5 mmol Ca/L, while the values of K, Mg and Na were an order of magnitude lower, ranging from 0.01 mmol/L to 0.4 mmol/L, as shown in Fig. 3.

The substantial concentration of Ca(II) in solution can be explained by the dissolution of CaO(s) particles present on the FA as described by Eq. 12:

$$\mathrm{CaO(s)} + H_2\mathrm{O} \quad \leftrightarrow \quad \mathrm{Ca(OH)_2(s)} \leftrightarrow \quad \mathrm{Ca^{2+}} + 2\mathrm{OH^-} \qquad (12)$$

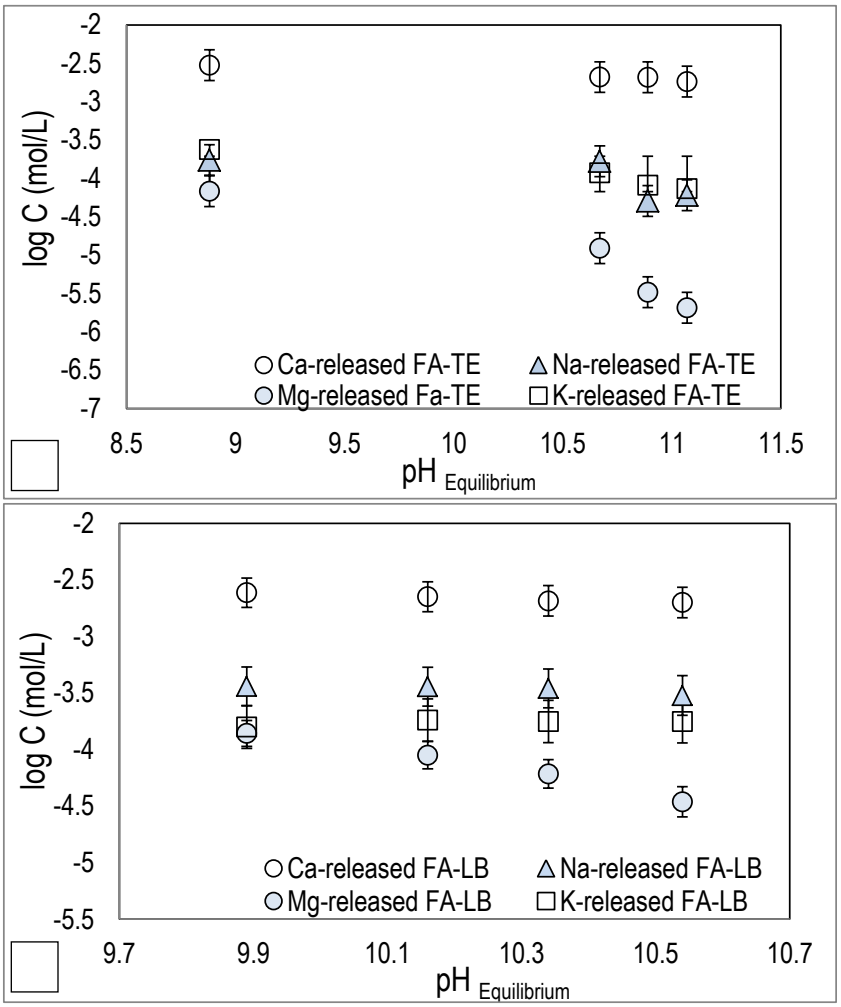

Figure 3. Molar Ca, Mg, Na and K concentration (in logarithm form) as a function of the equilibrium pH for the fly ash dissolution experiments (0.2 mass of FA and 10 mL volume of demineralized water) for both type of FA samples a) FA-TE and b) FA-LB.

The measured Ca(II) values decreases as pH increases as can be expected based on the CaO(s) dissolution reaction and the values are slightly higher for FA-TE, which has a higher Ca content (4.2% CaO). Although mineral phases containing Ca were detected in both FAs, Ca is expected to be present as calcium oxide minerals (e.g., portlandite) [48]. The measured concentrations of other major components of FA, such as Al, Fe, Si, and Ti, were below 0.01 mmol/L. These values are in accordance with the solubility data of the main mineral phases identified by XRD in both FA samples: quartz (SiO_2), mullite ($Al_6Si_2O_{12}$) and hematite (Fe_2O_3) (Fig. 1a).

3.2 Phosphate sorption capacities of FA-TE and FA-LB: Effects of pH and P(V) concentration

P(V) sorption isotherms for both FA samples revealed a dependence on the pH (Fig. 4), and the equilibrium data were well described by the Langmuir isotherm (Table 3). The maximum P(V) sorption capacities were 38.8±3.4 and 19.1±1.7mgP-PO_4 /g for FA-TE and FA-LB, respectively, when the pH values exceeded 7. At pH 8, the maximum uptakes were 59.5±4.3 and 54.1±3.7 mgP-PO_4/g for FA-TE and FA-LB, respectively. The P(V)-sorption capacities measured here are in the same order of magnitude with those reported by Chen et al. [47] as phosphate immobilization capacity in FA samples with CaO contents from 2 to 5% using an initial phosphate concentration of 1000 mgP-PO_4/L.

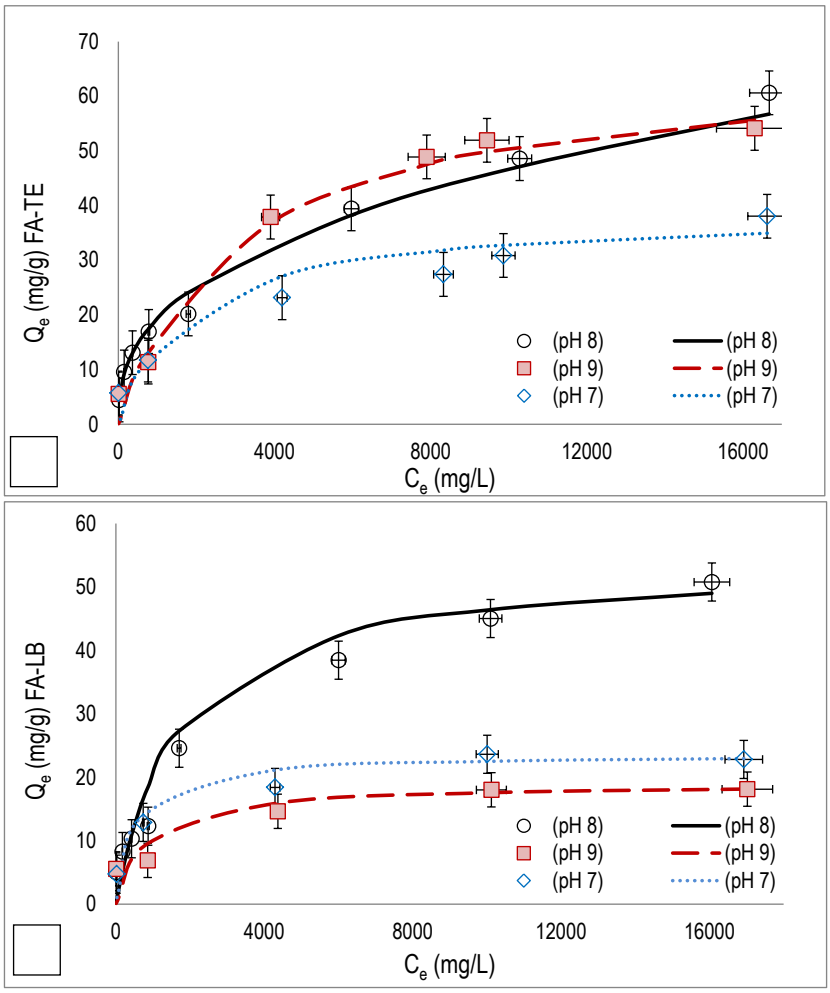

Figure 4. Phosphate sorption isotherms at different pH and predicted by the Langmuir model for a) FA-TE and b) FA-LB (dots: experimental data; line: the predicted values).

Table 3. Langmuir and Freundlich isotherm parameters for Teruel (FA-TE) and Los Barrios (FALB) fly ash samples at different pH values

Adsorbent / Models		FA-TE			FA-LB		
		pH 7	pH 8	pH 9	pH 7	pH 8	pH 9
Langmuir isotherm	q_m (mg/g)	38.8±3.4	59.5±4.3	56.2±3.8	23.7±2.3	54.1± 3.7	19.1±1.7
	K_L (L/mg)	0.0005	0.0005	0.0003	0.0019	0.0006	0.0015
	R^2	0.98	0.99	0.99	0.99	0.97	0.99

Freundlich isotherm	K_f (mg/g)/(mg/L)$^{1/n}$	4.9	1.4	2.9	2.4	1.8	3.8
	n	5.3	2.6	3.3	4.1	3,0	6.5
	R^2	0.91	0.95	0.89	0.85	0.92	0.81

3.3 P(V)-sorption mechanism on FA

Given that $H_2PO_4^-$ and HPO_4^{2-} are the predominant species of P(V) at pH values between 7 to 9, two main sorption mechanisms can be postulated:

a) Surface complexation with ≅AlOH and ≅FeOH functional groups of Al and Fe oxides through following reactions (Eqs.13-14):

Labile complexes with ≅MOH_2^+: ≅MOH_2^++$H_2PO_4^-$/HPO_4^{2-}↔ ≅$MOH_2^+H_2PO_4^-$/HPO_4^{2-} (13)

Inner-sphere complexes with ≅MOH: ≅MOH+$H_2PO_4^-$/HPO_4^{2-}↔ ≅$MH_2PO_4^-$/HPO_4^{2-}+OH (14)

where M represents Al or Fe.

b) Formation of Ca-phosphate minerals with Ca(II) ions present on the FA samples as CaO(s):

HPO_4^-/HPO_4^{2-}+CaO(s) = Ca-phosphates ($CaHPO_4$(s) or $Ca_5(OH)(PO_4)_3$ (s)) (15)

XRD analysis of FA samples after the sorption experiments revealed the presence of brushite ($CaHPO_4$(s)) at pH 7 and 8; the presence of Ca-phosphate minerals was not detected only at pH 9, as can be seen in Fig. 5. This could be due the formation of undetectable nanocrystals or amorphous structures because the removal rate at pH 9 is faster than those at pH 7 and 8, as indicates by the kinetic analysis (see section 4). Generally, precipitation processes with fast kinetics produce less-crystalline solids. In addition to hematite and/or maghemite, mullite and quartz were detected in all samples.

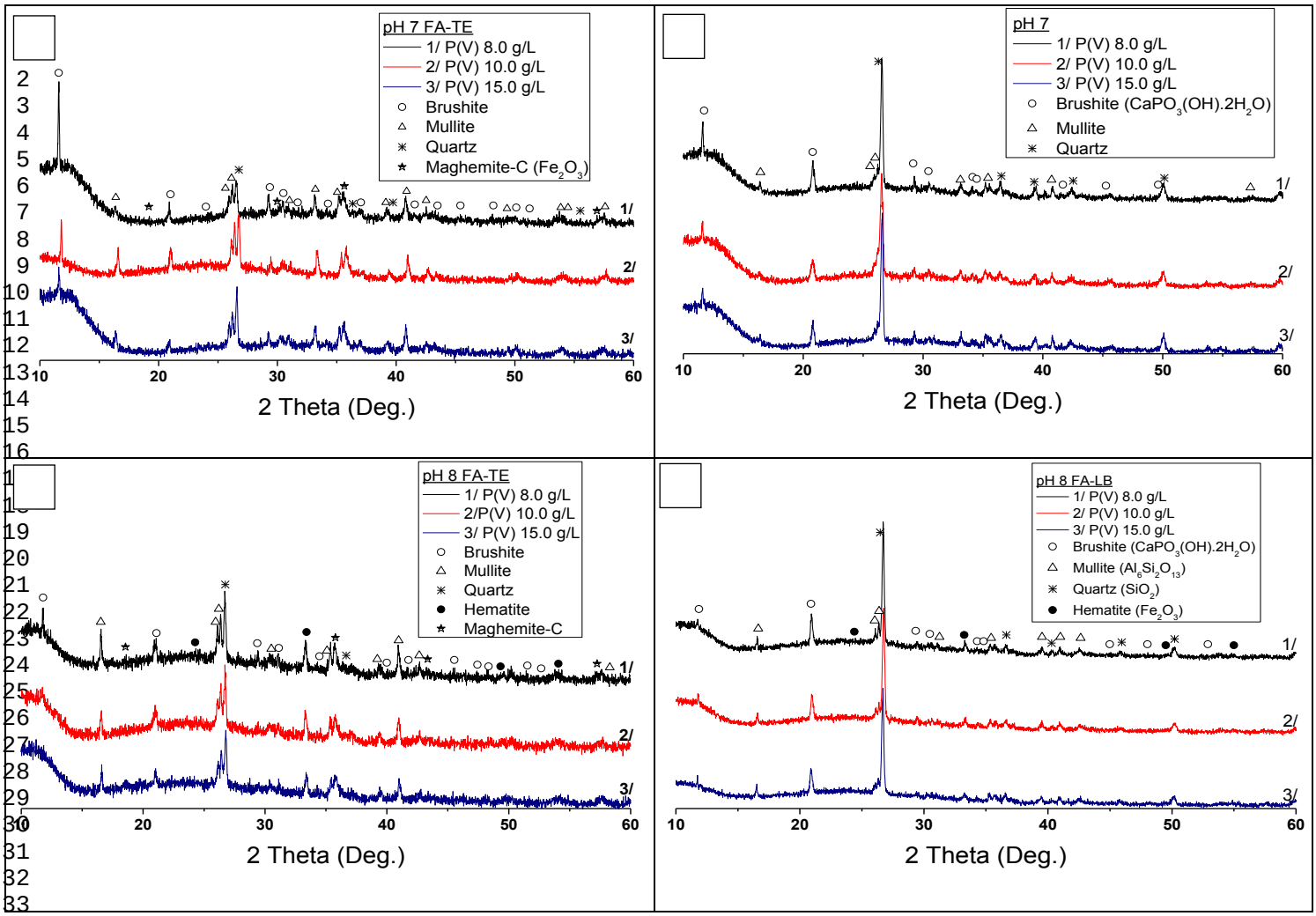

Figure 5. XRD analysis of fly ash samples after phosphate sorption at different pH values and for different phosphate concentrations for FA-TE (a-b) and FA-LB (c,d) FA samples.

The P-speciation analysis of loaded samples shown in Fig. S1 (Supplementary material) indicates that the loosely bound P fraction (KCl speciation fraction), associated with the labile complexes (Eq. 13) accounted for 18% in FA-TE and 4% in FA-LB. The Ca-Mg-speciation (HCl-P speciation fraction) associated with Ca-phosphate forms (Eq. 15), accounted for 81% in FA-TE and 95% in FA-LB. The NaOH–P fraction associated with P(V) bound to the hydrated metal oxides (Eq. 14) reported a residual contribution of less than 1%, while the residual P speciation represents less than 0.9%.

The formation of Ca-phosphates (e.g., brushite and Hap) is thermodynamically favoured under the studied conditions, as shown in Fig. S2 (Supplementary material); Hap is a more stable phase than

brushite, which is considered its precursor phase. However, as the reaction proceeds on the microporous FA structure under the controlled Ca(II) ion release provided by CaO(s) dissolution, which avoids oversaturation, and brushite is formed and then stabilised, stopping the conversion to Hap. Thus, the main P(V) sorption process can be postulated according to Eqs. 16-17:

$$Ca(OH)_2(s) + HPO_4^{2-} \leftrightarrow CaHPO_4(s) + 2OH^- \qquad \log K=32.2 \quad (25^{\circ}C) \quad (16)$$

$$Ca(OH)_2(s) + H_2PO_4^- \leftrightarrow CaHPO_4(s) + H_2O + OH^- \qquad \log K=22.2 \quad (25^{\circ}C) \quad (17)$$

The removal of P(V) as brushite is accompanied by a release of 1 to 2 moles of OH^- ions per mole of P(V), which increases the pH, as observed in the sorption tests. For both FA samples, the sorption capacity is maximised at pH 8 and decreases as the pH increases to 9 or decreases to 7. This sorption behaviour is in agreement with the formation of brushite. The solubility of brushite estimated by HYDRA-MEDUSA code (in logarithmic form) and the P(V) sorption capacity as a function of pH are plotted in Fig. 6. The minimum solubility, which corresponds to the highest brushite stability, is found at pH 8, where the maximum sorption capacities were also observed. Increasing or decreasing the pH increased the brushite solubility and accordingly decreased the P(V)-sorption capacity.

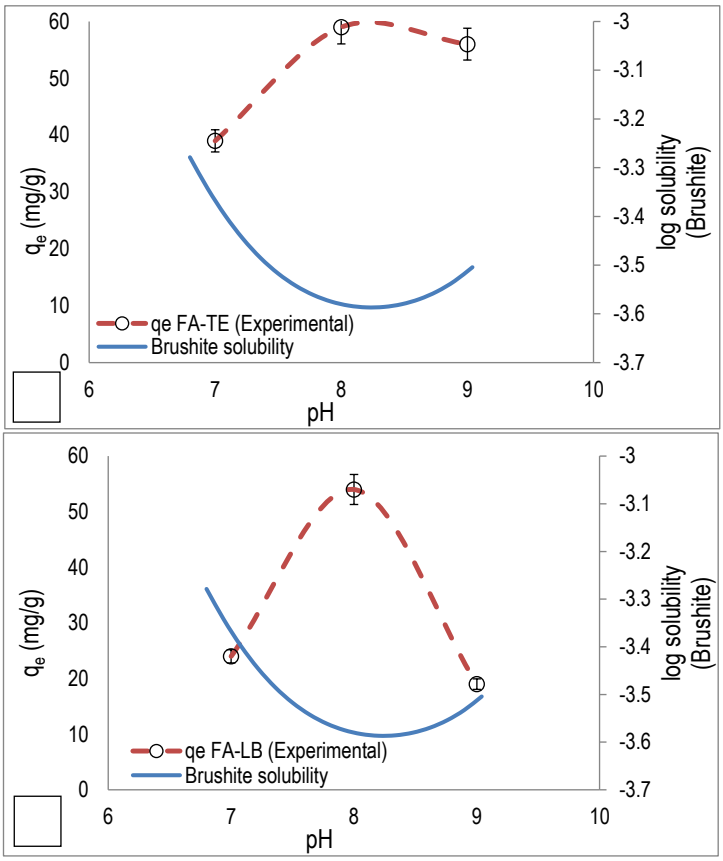

Figure 6. The experimental P(V) sorption capacity at different pH and the estimated curve of brushite solubility for a) FA-TE and b) FA-LB.

4. Phosphate sorption kinetics

The results of the kinetic experiments involving P(V) solutions containing 100 and 500 mgP-PO_4/L at an initial pH value of 8 are shown in Fig. 7a-b, and the evolution of the total Ca(II) concentration is presented in Fig. 7c. The sorption profiles with time exhibit decreased phosphate and Ca(II) concentrations and increased pH values. For the kinetic test at 500 mg P-PO_4/L, the sorption rates of both FA samples (Fig. 7a-7b) are quite similar as it is controlled by the excess phosphate relative to the Ca(II) provided by the FA. The sorption process can be divided into a first, faster step and a second, slower one. Initially, phosphate rapidly reached the boundary layer to interact with dissolved Ca(II) ions from the CaO(s) grains [49,50], and then, it slowly diffused from the boundary layer film onto the FA particle. At that time, P(V) removal was coupled with CaO(s) dissolution [51], which supplied the

reactant needed to facilitate brushite formation [16,52]. The evolution of Ca(II) for both FA samples in the kinetic experiments with 100 and 500 mgP-PO_4/L (Fig. 7c) revealed that the total Ca(II) concentration follows a profile very similar to that of the total P(V) concentration (Fig. 7a). The total Ca(II) and P(V) concentrations and the measured pH were used to determine the saturation indexes for brushite and Hap. The saturation index values (data not shown) indicated that the system was oversaturated in Hap; however, as discussed previously, its precursor, brushite, was the only mineral phase identified by XRD analysis in this study.

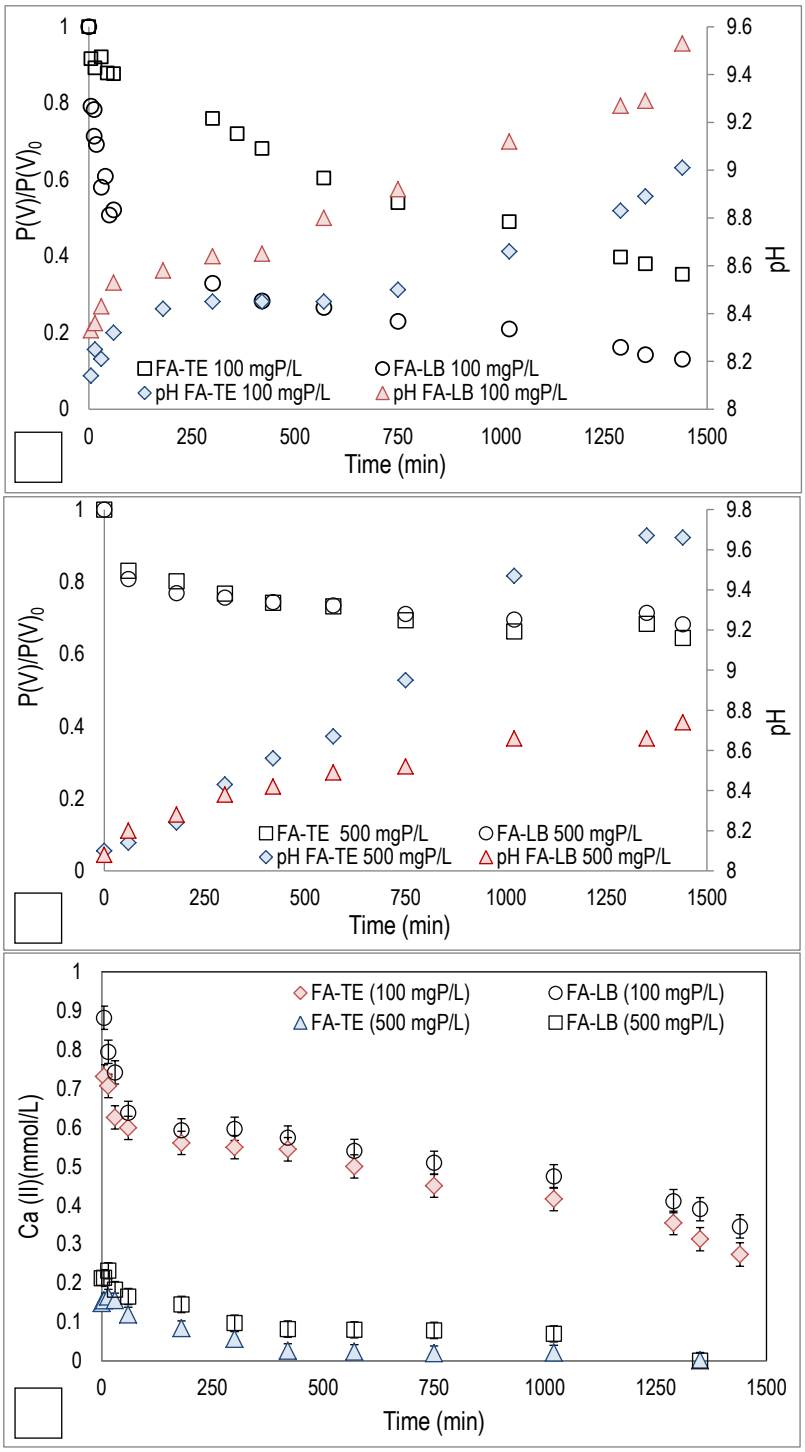

Figure 7. Variation of ratio $P(V)/P(V)_0$ and pH as a function of time for an initial concentration a) 100 mg/L , b) 500 mg/L at initial pH= 8 and c) variation of Ca(II) concentration as a function of contact time for an initial P(V) concentration of 100 and 500 mg/L, at initial pH= 8 (sorbent dose: 0.2 g/10 mL).

The influence of the initial pH on the kinetics of both FA samples with 100 mgP/L phosphate solutions is shown in Fig. 8. The $P(V)/P(V)_0$ ratio profiles with time for both FA samples (Fig. 8a, 8b) are strongly

affected by pH, especially that of FA-LB. As the extraction reaction proceeds, the pH increases, as described by Eqs. 16-17 and shown in Fig. 8b-8d. Experiments at pH values of 7-8 exhibited greater increases (ΔpH>0.5 units) than that at pH 9 because of their lower buffer capacities (ΔpH<0.5 units).

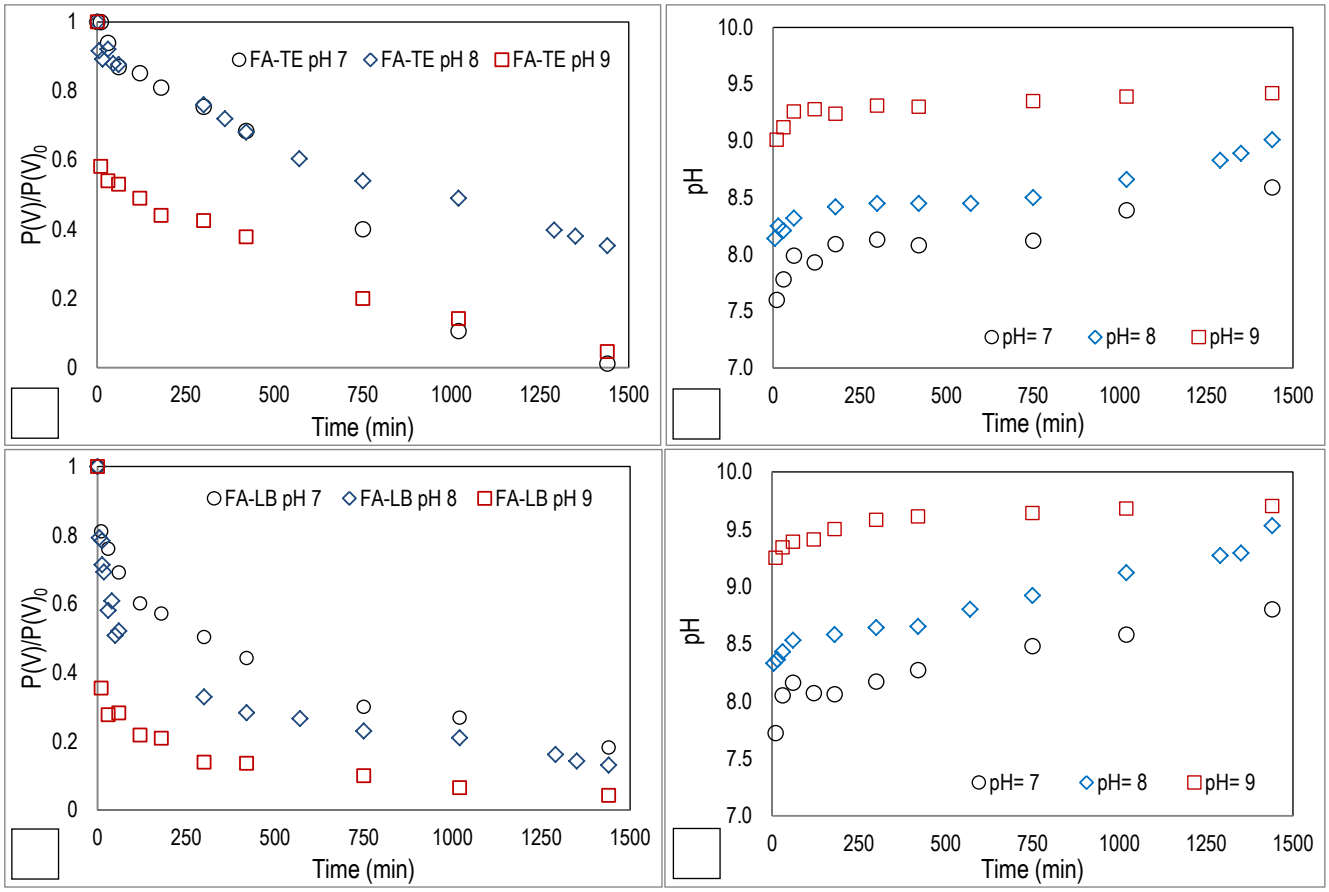

Figure 8. Variation of $P(V)/P(V)_0$ ratio for a) FA-TE and c) FA-LB samples, and pH as a function of contact time for an initial concentration of 100 mg $P\text{-}PO_4/L$ (sorbent dose: 0.2 g/10 mL) for b) FA-TE and d) FA-LB samples.

For FA-LB, most of the phosphate removal was achieved in the first 120 min: 40% at pH 7 to 80% at pH 9. In contrast, FA-TE exhibited a lower sorption rate, and longer contact times (more than 1000 minutes) were therefore required to reach equilibrium values. These differences are connected with the

compositions of the FA samples, including the SiO_2 and Al_2O_3 contents and especially that of mullite, which can be adjusted to improve their hydrophilic properties.

4.1 Sorption kinetic modelling results

The results of the kinetic modeling of phosphate sorption onto FA are shown in Fig. S3 (Supplementary material). Kinetic data fitting results in Eqs. 5-6 using the HPDM and Eqs. 8-10 for the SPM, are summarized in Table 4. The linear correlation coefficients indicate that film diffusion can be discarded as the sorption-controlling step because data did not exhibit a linear dependence. Both models fit the data satisfactorily for the entire time range of FA-phase diffusion.

Table 4. Linear regression of HPDM and SPM models for phosphate sorption for initial concentration of 100 mgP-PO_4/L at different initial pH conditions onto FA samples

		HPDM						SPM					
		-ln (1-X^2)				-ln (1-X)		X		(3-3(1-X)$^{2/3}$-2X)		(1-(1-X)$^{1/3}$)	
	pH_i	$pH_{t,m}$	R^2	D_e		R^2	D	R^2	K_F	R^2	D_e	R^2	k_s
FA-TE	7	(8.0)*	0.99	$3.3\ 10^{-15}$		0.94	$1.1\ 10^{-9}$	0.78	$2.9\ 10^{-10}$	0.99	$3.6\ 10^{-15}$	0.93	$7.1\ 10^{-12}$
	8	(8.3)*	0.98	$6.7\ 10^{-16}$		0.91	$2.2\ 10^{-10}$	0.90	$7.6\ 10^{-11}$	0.98	$7.6\ 10^{-16}$	0.93	$1.3\ 10^{-12}$
	9	(9.2)*	0.98	8.110^{-16}		0.96	$2.3\ 10^{-10}$	0.89	$5.5\ 10^{-11}$	0.98	$1.2\ 10^{-15}$	0.95	2.310^{-12}
FA-LB	7	(8.2)*	0.99	$8.6\ 10^{-16}$		0.95	$2.7\ 10^{-10}$	0.88	$1.5\ 10^{-10}$	0.99	$1.3\ 10^{-15}$	0.97	$2.3\ 10^{-12}$
	8	(8.5)*	0.97	$5.0\ 10^{-15}$		0.87	$4.8\ 10^{-10}$	0.74	$5.9\ 10^{-11}$	0.97	$6.4\ 10^{-15}$	0.89	$2.1\ 10^{-12}$
	9	(9.3)*	0.99	$3.7\ 10^{-15}$		0.92	$4.1\ 10^{-10}$	0.85	$7.3\ 10^{-11}$	0.97	$5.1\ 10^{-15}$	0.91	$1.9\ 10^{-12}$

* Values in brackets are the pH along the kinetic test with time t and specific point m.

The predicted curves obtained using both models for FA-LB and FA-TE at different initial pH values are shown in Fig. S3 a - b (Supplementary material). FA-TE and FA-LB showed better agreement (between the predicted and experimental data) at pH 7 and 8 than at pH 9. Taking into account the fact that the

pH changes as a consequence of the sorption process along the kinetic experiments (Fig. 8 b and d), the $H_2PO_4^-/HPO_4^{2-}$ molar ratio (%) is 12/88 at pH 8.2 and 1/99 at pH 9.5; therefore, the effective diffusion coefficient can be considered to accounts for a single species (HPO_4^{2-}).

5. Evaluation of phosphate availability from loaded FA samples

Olsen et al. [53] suggested bicarbonate extraction as a suitable method for predicting the plant availability of phosphate in calcareous soils where the main role of $NaHCO_3$ in phosphate extraction is decreasing the Ca(II) activity by forming $CaCO_3$. The phosphate-availability data in solutions of 0.5 M $NaHCO_3$ are plotted in Fig. 9 as a function of the extracted amount of phosphate by FA (mgP-PO_4/g FA). For both FA samples, ratios from 8 to 30 mgP-PO_4/g FA were obtained. Partial extraction of 20 to 70% was reported in a single-extraction trial for both FA samples.

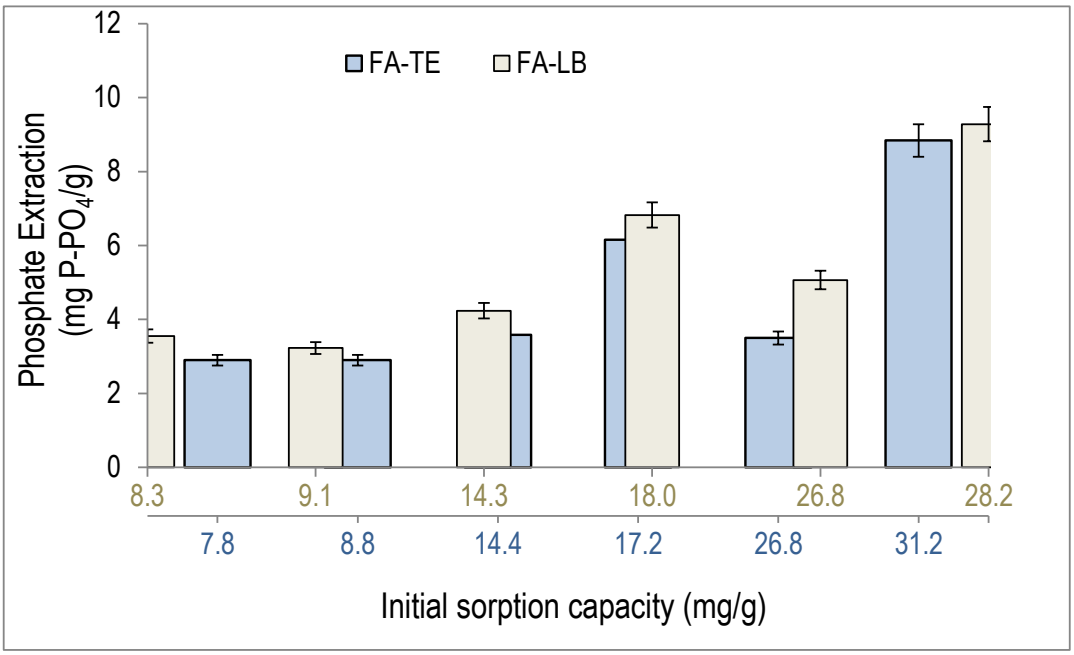

Figure 9. Phosphate extraction using mixture of $NaHCO_3$ (0.2M) from loaded fly ash samples (a) FA-TE and (b) FA-LB

These results are in good agreement with the speciation results reported in Fig. S1 (Supplementary material). In the presence of excess of bicarbonate, the labile phosphate fraction (P-KCl) will be displaced by bicarbonate ions, and partial brushite dissolution will be achieved according to Eq. 18:

$$CaHPO_4(s) + HCO_3^- \leftrightarrow CaCO_3(s) + H_2PO_4^- \qquad \log K=-1.3 \quad (25ºC) \quad (18)$$

The sorbed P(V) on FA samples has been demonstrated to dissolve in solutions containing moderate to high bicarbonate concentrations similar to those expected in basic soils characterised by a high content of calcareous rocks (e.g., limestone) and where other Ca-phosphate minerals, such as Hap, are very insoluble and then with limited plant availability.

6. Conclusions

The P(V)-removal results in the expected pH range (6 to 9) of wastewater effluents indicated that sorption proceeds via a diffusion-controlled process involving phosphate ions within the FA particles coupled with CaO(s) dissolution from the FA, which provides the Ca(II) ions required for brushite ($CaHPO_4(s)$) formation. This process is important because it avoids the formation of relatively insoluble Ca-phosphates, such as Hap, which have more limited fertilizing properties. P(V) availability from loaded FAs was determined using $NaHCO_3$ solutions and revealed P(V)-release ratios of 10 to 30 gP-PO_4/g FA. In addition, phosphate removal is highly efficient as indicated by the rapid removal and high P-loadings obtained (up to 50 mgP-PO_4/g FA (5%P(V) by weight) at pH 8.

The use of phosphate-containing mineral-based sorbents as soil amendments may be advantageous when other agronomic benefits are expected, such as the provision of other plant nutrients or the enhancement of the soil moisture-holding capacity.

Future research should be performed to scale this process up from the laboratory scale to pilot- and full-scale systems integrating sorption and ultrafiltration membrane filtration and to evaluate other types of powdered Ca-rich inorganic sorbents for phosphate removal and direct use as fertilizer. The study on the transfer of trace heavy metals ions and non-metal ions to the treated waters and the potential

transfer from loaded FA to soils when applied as fertilizers will be needed to approve its potential uses by environmental and agricultural regulation agencies.

Acknowledgments

This study has been supported by the ZERODISCHARGE project (CTQ2011-26799) and the Waste2Product project (CTM2014-57302-R) financed by Ministry of Science and Innovation (MINECO, Spain) and the Catalan government (project ref. 2014SGR050). R. Estany (Aigues de Barcelona) and M. Gullom (EMMA) and I. Sancho (Centro Tecnologíco del Agua (CETAQUA)) for waste water samples supply.

7. References

[1] K.S. Hui, C.Y.H. Chao, Effects of step-change of synthesis temperature on synthesis of zeolite 4A from coal fly ash, Microporous Mesoporous Mater. 88 (2006) 145–151.

[2] J. Yan, D.W. Kirk, C.Q. Jia, X. Liu, Sorption of aqueous phosphorus onto bituminous and lignitous coal ashes., J. Hazard. Mater. 148 (2007) 395–401.

[3] P. Pengthamkeerati, T. Satapanajaru, P. Chularuengoaksorn, Chemical modification of coal fly ash for the removal of phosphate from aqueous solution, Fuel. 87 (2008) 2469–2476.

[4] N. Lior, Sustainable energy development: The present (2009) situation and possible paths to the future, Energy. 35 (2010) 3976–3994.

[5] Z.T. Yao, X.S. Ji, P.K. Sarker, J.H. Tang, L.Q. Ge, M.S. Xia, Y.Q. Xi, A comprehensive review on the applications of coal fly ash, Earth-Science Rev. 141 (2015) 105–121.

[6] U. Bhattacharjee, T.C. Kandpal, Potential of fly ash utilisation in India, Energy. 27 (2002) 151–166.

[7] C.F. Wang, J.S. Li, L.J. Wang, X.Y. Sun, Influence of NaOH concentrations on synthesis of pure-form zeolite A from fly ash using two-stage method, J. Hazard. Mater. 155 (2008) 58–64.

[8] R.P. Penilla, A. Guerrero Bustos, S. Goñi Elizalde, Immobilization of Cs, Cd, Pb and Cr by synthetic zeolites from Spanish low-calcium coal fly ash, Fuel. 85 (2006) 823–832.

[9] D. Wu, B. Zhang, C. Li, Z. Zhang, H. Kong, Simultaneous removal of ammonium and phosphate by zeolite synthesized from fly ash as influenced by salt treatment, J. Colloid Interface Sci. 304 (2006) 300–306.

[10] L.E. de-Bashan, Y. Bashan, Recent advances in removing phosphorus from wastewater and its future use as fertilizer (1997-2003)., Water Res. 38 (2004) 4222–46.

[11] J. Ma, L. Zhu, Simultaneous sorption of phosphate and phenanthrene to inorgano-organo-bentonite from water, J. Hazard. Mater. 136 (2006) 982–988.

[12] S.G. Lu, S.Q. Bai, L. Zhu, H.D. Shan, Removal mechanism of phosphate from aqueous solution

by fly ash, J. Hazard. Mater. 161 (2009) 95–101.

[13] G. Zelmanov, R. Semiat, The influence of competitive inorganic ions on phosphate removal from water by adsorption on iron (Fe^{+3}) oxide/hydroxide nanoparticles-based agglomerates, J. Water Process Eng. 5 (2014) 143–152.

[14] C.A. Gray, A.P. Schwab, Phosphorus-fixing ability of high ph, high calcium, coal-combustion, waste materials, Water. Air. Soil Pollut. 69 (1993) 309–320.

[15] R. Tsitouridou, J. Georgiou, A contribution to the study of phosphate sorption by three Greek fly ashes, Toxicol. Environ. Chem. 17 (1988) 129–138.

[16] M. Ahmaruzzaman, A review on the utilization of fly ash, Prog. Energy Combust. Sci. 36 (2010) 327–363.

[17] D.G. Grubb, M.S. Guimaraes, R. Valencia, Phosphate immobilization using an acidic type F fly ash, J. Hazard. Mater. 76 (2000) 217–236.

[18] K.C. Cheung, T.H. Venkitachalam, Improving phosphate removal of sand infiltration system using alkaline fly ash, Chemosphere. 41 (2000) 243–249.

[19] L. Johansson, J.P. Gustafsson, Phosphate removal using blast furnace slags and opoka-mechanisms, Water Res. 34 (2000) 259–265.

[20] M. Parvinzadeh Gashti, M. Stir, M. Bourquin, J. Hulliger, Mineralization of Calcium Phosphate Crystals in Starch Template Inducing a Brushite Kidney Stone Biomimetic Composite, Cryst. Growth Des. 13 (2013) 2166–2173.

[21] S. V. Dorozhkin, Self-Setting Calcium Orthophosphate Formulations: Cements, Concretes, Pastes and Putties, Int. J. Mater. Chem. 1 (2012) 1–48.

[22] X. Liu, C. Ding, Morphology of apatite formed on surface of wollastonite coating soaked in simulate body fluid, Mater. Lett. 57 (2002) 652–655.

[23] Y. Watanabe, T. Ikoma, H. Yamada, G.W. Stevens, Y. Moriyoshi, J. Tanaka, Y. Komatsu, Formation of hydroxyapatite nanocrystals on the surface of Ca-Al-layered double hydroxide, J. Am. Ceram. Soc. 93 (2010) 1195–1200.

[24] J.Z. Zhou, L. Feng, J. Zhao, J. Liu, Q. Liu, J. Zhang, G. Qian, Efficient and controllable phosphate removal on hydrocalumite by multi-step treatment based on pH-dependent precipitation, Chem. Eng. J. 185–186 (2012) 219–225.

[25] D. Guaya, C. Valderrama, A. Farran, C. Armijos, J.L. Cortina, Simultaneous phosphate and ammonium removal from aqueous solution by a hydrated aluminum oxide modified natural zeolite, Chem. Eng. J. 271 (2015) 204–213.

[26] K. Xu, T. Deng, J. Liu, W. Peng, Study on the phosphate removal from aqueous solution using modified fly ash, Fuel. 89 (2010) 3668–3674.

[27] N. Moreno, X. Querol, J. Andres, K. Stanton, M. Towler, H. Nugteren, M. Janssenjurkovicova, R. Jones, Physico-chemical characteristics of European pulverized coal combustion fly ashes, Fuel. 84 (2005) 1351–1363.

[28] R.E. Kitson, M.G. Mellon, Colorimetric determination of phosphorus as molybdovanadophosphoric acid, Ind. Eng. Chem. Anal. 16 (1944) 379-383.

[29] M.J.Hedley, J.W. B Stewart, B.S. Chauhan, Changes in Inorganic and Organic Soil Phosphorus Fractions Induced by Cultivation Practices and by Laboratory Incubations, Soil.Sci.AM.J. 46 (1982) 970–976.

[30] Y. Ann, K.R. Reddy, J.J. Delfino, Influence of chemical amendments on phosphorus immobilization in soils from a constructed wetland, 14 (2000) 157–167.

[31] S. Moharami, M. Jalali, Phosphorus leaching from a sandy soil in the presence of modified and un-modified adsorbents., Environ. Monit. Assess. 186 (2014) 6565–76.

[32] X. Querol, M.K.G. Whateley, J.L. Fernández-Turiel, E. Tuncali, Geological controls on the mineralogy and geochemistry of the Beypazari lignite, central Anatolia, Turkey, Int. J. Coal Geol. 33 (1997) 255–271.

[33] K. Skartsila, N. Spanos, Surface characterization of hydroxyapatite: Potentiometric titrations coupled with solubility measurements, J. Colloid Interface Sci. 308 (2007) 405–412. doi:10.1016/j.jcis.2006.12.049.

[34] Y. Liu, R. Naidu, H. Ming, Surface electrochemical properties of red mud (bauxite residue): zeta potential and surface charge density, J Colloid Interface Sci. 394 (2013) 451–457.

[35] H.R. Zebardast, M. Pawlik, S. Rogak, E. Asselin, Potentiometric titration of hematite and magnetite at elevated temperatures using a ZrO2-based pH probe, Colloids Surfaces A Physicochem. Eng. Asp. 444 (2014) 144–152.

[36] R.E. Martinez, O.S. Pokrovsky, J. Schott, E.H. Oelkers, Surface charge and zeta-potential of metabolically active and dead cyanobacteria, J. Colloid Interface Sci. 323 (2008) 317–325.

[37] K.Y. Foo, B.H. Hameed, Insights into the modeling of adsorption isotherm systems, Chem. Eng. J. 156 (2010) 2–10.

[38] X. You, A. Farran, D. Guaya, C. Valderrama, V. Soldatov, J.L. Cortina, Phosphate removal from aqueous solutions using a hybrid fibrous exchanger containing hydrated ferric oxide nanoparticles, J. Environ. Chem. Eng. 4 (2016) 388–397.

[39] Y.M. (Eds) L. Liberti, R. Passino, in : J.A. Marinsky, Ion Exchange and Solvent Extraction, 1977. doi:10.1016/S0304-386X(02)00007-5.

[40] I.S.S. Puidomènech, Chemical Equilibrium Software Hydra and Medusa, Stock. Sweden. (2001) Inorganic Chemistry Department.Stock. Sweden.

[41] J.E. Gray-Munro, M. Strong, A study on the interfacial chemistry of magnesium hydroxide surfaces in aqueous phosphate solutions: influence of Ca^{2+}, Cl^{-} and protein., J. Colloid Interface Sci. 393 (2013) 421–428.

[42] M. Sarkar, P.K. Acharya, Use of fly ash for the removal of phenol and its analogues from contaminated water, Waste Manag. 26 (2006) 559–570.

[43] J. Schwarz, C. Driscoll, A . Bhanot, The zero point of charge of silica—alumina oxide suspensions, J. Colloid Interface Sci. 97 (1984) 55–61.

[44] T.S. Malarvizhi, T. Santhi, S. Manonmani, A Comparative Study of Modified Lignite Fly Ash for the Adsorption of Nickel from Aqueous Solution by Column and Batch Mode Study, 3 (2013) 44–53.

[45] B.-H. Zhang, D.-Y. Wu, C. Wang, S.-B. He, Z.-J. Zhang, H.-N. Kong, Simultaneous removal of ammonium and phosphate by zeolite synthesized from coal fly ash as influenced by acid treatment., J. Environ. Sci. (China). 19 (2007) 540–5.

[46] B. B. E. Reed, ASCER. Member, R. Vaughan , L. Jiang, As (III), As (V), Hg and removal by Fe-Oxide impregnated activated carbon. J. Environ .Eng. 126 (2000) 869–873

[47] J. Chen, H. Kong, D. Wu, Z. Hu, Z. Wang, Y. Wang, Removal of phosphate from aqueous solution by zeolite synthesized from fly ash., J. Colloid Interface Sci. 300 (2006) 491–7.

[48] R. Hooton, J. Tishmack, J. Olek, S. Diamond, Characterization of High-Calcium Fly Ashes and Their Potential Influence on Ettringite Formation in Cementitious Systems, Cem. Concr. Aggregates. 21 (1999) 82.

[49] J.L. Cortina, I. Lagreca, J. De Pablo, J. Cama, C. Ayora, Passive in situ remediation of metal-polluted water with caustic magnesia: Evidence from column experiments, Environ. Sci. Technol. 37 (2003) 1971–1977.

[50] T.S. Rotting, C. Ayora, J. Carrera, Improved Passive Treatment of High Zn and Mn Concentrations Using Caustic Magnesia (MgO): Particle Size Effects Improved Passive Treatment of High Zn and Mn Concentrations Using Caustic Magnesia (MgO): Particle Size Effects, 42 (2008) 9370–9377.

[51] L. Bernard, M. Freche, J.L. Lacout, B. Biscans, Modeling of the dissolution of calcium hydroxide in the preparation of hydroxyapatite by neutralization, Chem. Eng. Sci. 55 (2000) 5683–5692.

[52] C. Barca, C. Gérente, D. Meyer, F. Chazarenc, Y. Andrès, Phosphate removal from synthetic and real wastewater using steel slags produced in Europe., Water Res. 46 (2012) 2376–2384.

[53] L. Olsen, S.R. ; Cole, C.V; Watanabe, F.S; Dean, Estimation Of Available Phosphorus In Soils By Extraction With Sodium Bicarbonate, United Sta, United States Department Of Agriculture ; Washington, 1954.